

Tandem Reactivity of a Self-Assembled Cage Catalyst with Endohedral Acid Groups

Lauren R. Holloway, Paul M. Bogie, Yana Lyon, Courtney Ngai, Tabitha F. Miller, Ryan R. Julian,^{1b} and Richard J. Hooley*^{1b}

Department of Chemistry, University of California–Riverside, Riverside, California 92521, United States

S Supporting Information

ABSTRACT: Self-assembly of a carboxylic acid-containing ligand into an Fe_4L_6 iminopyridine cage allows endohedral positioning of the acid groups while maintaining a robust cage structure. The cage is an effective supramolecular catalyst, providing up to 1000-fold rate enhancement of acetal solvolysis. This enhanced reactivity allows a tandem deprotection/cage-to-cage interconversion that cannot be achieved with other acid catalysts. The combination of rate enhancements and sequestration of the reactive function confers both activity and selectivity on the process, mimicking enzymatic behavior.

Biomimetic catalysis with self-assembled cage complexes¹ is a long-standing target, whether the cages are based on self-complementary hydrogen bonds,² hydrophobic forces³ or metal–ligand interactions.⁴ As the inner shells of most self-assembled cages are unfunctionalized, the most effective reactions are reagentless, either unimolecular rearrangements or cycloadditions.⁵ In some special cases, the host superstructure can be involved in the reaction: electron-rich aromatic panels can participate in internal substitution reactions,⁶ charged cages can exploit localized hydroxide ions to accelerate pH-responsive reactions,⁷ and acidic CH bonds in the architecture allow guest activation.⁸

Cages with endohedrally oriented functional groups would allow reagent-controlled reactions to be performed on the cavity interior. Functionalized cages could also perform reactions that are incompatible with the external milieu, or sequester reactive species, allowing compartmentalization and tandem processes.⁹ The challenge lies in the synthesis: presenting functionality to the interior of a self-assembled cage complex is still quite rare. Most examples are supercontainers or nanospheres with large internal spaces.¹⁰ Some of these large systems have been used to promote internal reactions, such as Au-catalyzed cyclizations controlled by cooperativity between bound substrates and internal groups.¹¹ Also, metal–organic supercontainers¹² with amine-functionalized walls can catalyze internal Knoevenagel condensations.¹³ However, in each case, the cavities are extremely large and selectivity in guest binding can be limited; they are better described as discrete nanophases^{10a} rather than biomimetic hosts.

To synthesize cages with reactive endohedral groups, ensuring compatibility between the catalytic group and

“structural” M–L interaction is essential. Appending unreactive groups is not an issue, but carboxylic acids are good ligands for metals, and are the structural components of many metal–organic frameworks.¹⁴ Fortunately, Fe(II)-iminopyridine-based self-assembly is tolerant to similar groups such as sulfates.¹⁵ Here we describe the synthesis of an Fe_4L_6 tetrahedral cage with internalized acid groups, and its application toward tandem catalytic processes.

A number of factors must be addressed when creating a tetrahedral assembly for supramolecular catalysis. The ligand must be large enough to allow a suitably sized cavity, as well as possessing the correct coordination angle. Linear ligands favor tetrahedral structures, but do not allow simple internalization of functional groups. V-shaped ligands allow endohedral functions,¹⁶ but invariably favor assemblies with a smaller, and entropically favored M_2L_3 stoichiometry.¹⁷ Also, the use of octahedral metals can lead to metal- and ligand-based stereoisomerism.¹⁸ 2,7-Diaminofluorene has been shown to assemble into an isomeric mixture of M_4L_6 tetrahedra,¹⁸ although the cavity is too small for effective molecular recognition. The coordination angle is ideal, however, so we focused on an extended 2,7-dianilino-fluorene scaffold for the creation of a functionalized cage (Figure 1). Two ligands were synthesized, unfunctionalized **C**, and diacid **E**. Suzuki coupling between **A** and 4-boc-aminophenylboronic acid, followed by deprotection gives **C** in 84% yield. To access the acid ligand, **A** was treated with α -bromoethyl acetate and KO^tBu , giving diester **B**. Suzuki coupling, Boc removal and hydrolysis of the esters followed by neutralization gave ligand **E** in 43% overall yield (4 steps).

Ligands **C** and **E** were treated with 2-formylpyridine (PyCHO) and $\text{Fe}(\text{NTf}_2)_2$ in acetonitrile, to give cages **1** and **2**, respectively. ESI-MS analysis of cage **2** showed only peaks for ions corresponding to an Fe_4L_6 stoichiometry, plus fragments (Figure 2a, see Table S-2 for full assignment). The dominant peak was for $[\text{2-1H}]^{7+}$, with other ions $[\text{2-2H}]^{6+}$ and $[\text{2-3H}]^{5+}$ present, indicating that the acids in cage **2** are generally protonated, despite the overall cationic nature of the cage. The ESI-MS spectrum for **1** gave similar stoichiometry, with a $[\text{1}]^{8+}$ base peak and peaks for the $[\text{1-NTf}_2]^{7+}$ and $[\text{1-(NTf}_2)_4]^{4+}$ ions (plus fragments) clearly observable (Figure S-24).

Both cages **1** and **2** displayed somewhat complex ^1H NMR spectra indicative of the formation of multiple cage isomers.

Received: April 13, 2018

Published: June 18, 2018

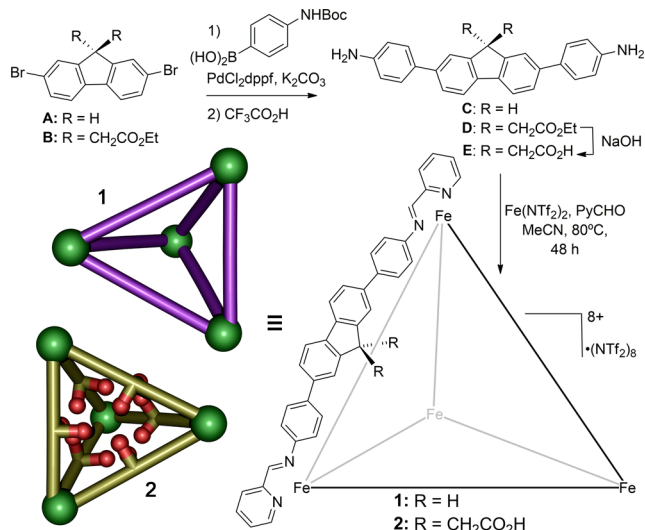


Figure 1. Ligand synthesis and multicomponent self-assembly into tetrahedral cage complexes **1** and **2**.

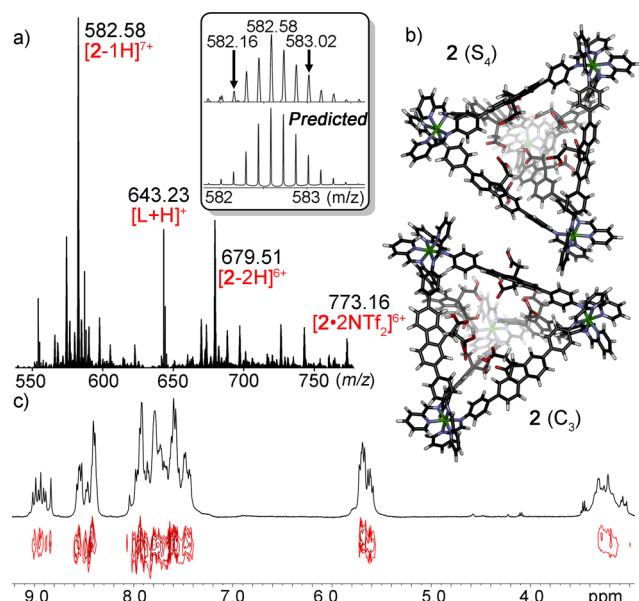


Figure 2. Characterization of cage **2**. (a) ESI-MS spectrum (L = ligand); (b) calculated energy minimized structures of the two observed isomers of **2** (C₃, S₄); (c) ¹H and 2D-DOSY NMR spectra (600 MHz, 298 K, CD₃CN, D(**2**) = 3.09 × 10⁻¹⁰ m/s²).

The spectrum of **2** (Figure 2c) shows discrete peaks in each expected region of the spectrum, but these peaks are overlapped and clustered. There are a variety of stereochemical possibilities for M₄L₆ tetrahedral structures. The most common is an all-*fac* coordination at the metal centers, giving rise to three isomeric possibilities, with either S₄, C₃, or T symmetry.¹⁹ Other possibilities exist with *mer* coordination at the metal center, but these show far more complex NMR spectra.²⁰ Deconvolution of the imine region of the ¹H NMR spectrum of cage **2** (Figure 3) shows the presence of only two isomers 2-C₃ (45%) and 2-S₄ (55%), with no observed peaks for the T-symmetric isomer. The unfunctionalized cage **1** shows 8 peaks in the imine region, with the extra peak corresponding to the T-symmetric isomer. The isomeric ratio is 48% 1-C₃, 11% 1-T, and 41% 1-S₄. 2D NMR and elemental

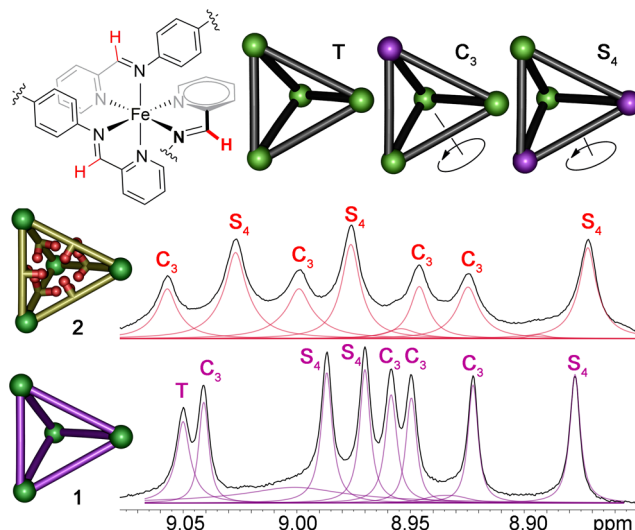


Figure 3. Peak deconvolutions of the downfield (imine CH) regions of the ¹H NMR spectra of **1** and **2** (600 MHz, 298 K, CD₃CN).

analysis (see Supporting Information) corroborates the assignment, as do the DOSY NMR spectra. All peaks for both **1** and **2** diffuse at the same rate, and the diffusion constants are nearly identical (D(**1**) = 3.01 × 10⁻¹⁰ m/s², D(**2**) = 3.09 × 10⁻¹⁰ m/s²).

Molecular modeling (semiempirical, AM1 force field) of the two isomers of acid **2** (Figure 2b) shows that in both cases, the acid groups are mostly positioned toward the internal cavity, and that rotation of the fluorenyl groups to exohedrally orient the acids is unfavorable. NOESY NMR shows intraligand NOE correlations that are likely due to free rotation of the phenyl spacers. This does not rule out rotation of the fluorenyl moiety, but if any rotation does occur, the barrier is low, and the acids can easily be oriented to the cavity interior at 23 °C (for further structural discussion, see Supporting Information). As such, cage **2** passes the first test: it has acidic groups on the ligands, and they can be oriented endohedrally. Is it capable of exploiting these reactive groups for biomimetic catalysis?

The challenge in using Fe-iminopyridine cages as catalysts is that they can be somewhat fragile. Strongly coordinating anions (e.g., Cl⁻) and other exogenous nucleophiles are rarely tolerated,^{16,21} so to determine the effectiveness of **2** as a catalyst, we initially focused on a mild acetal hydrolysis (Table 1). Aromatic acetals such as **3a–c** were treated with 4% cage **2** and 6 equiv of water in CD₃CN, and the reaction monitored by NMR. Solvolysis of **3a** was rapid in the presence of cage **2**, with 99% conversion after 5 h at 23 °C. The pyridyl equivalent **3b** was less reactive, and required heating to 77 °C for 14 h for complete reaction. No decomposition of cage **2** was detected during the solvolysis, and the cage-catalyzed reactions showed significant rate enhancements over control processes. The initial rates of the catalyzed hydrolyses of **3a** and **3b** were determined to be *V* = 2410 and 440 × 10⁻⁴ mM/min, respectively. Dibutylacetal **3c** was solvolyzed at the same rate as dimethyl acetal **3b**: cage **2** cannot discriminate between molecules of broadly similar size, due to its large cavity. When 6 equiv of control ligand **F** (i.e., an equivalent number of COOH groups as used with **2**) were used as catalyst, only 1% conversion of **3a** was observed after 24 h at 23 °C, with *V* = 2.26 × 10⁻⁴ mM/min. Only 20% conversion was observed when heated at 50 °C for an additional 24 h. Similarly, **3b** only

Table 1. Supramolecular Catalysis of Acetal Solvolysis

3a: X=CH, R=Me
3b: X=N, R=Me
3c: X=N, R=n-Bu

4% Catalyst
6 eq. H₂O
CD₃CN

Catalysts:

Substrate ^a	t, h	T, °C	Catalyst ^b	Initial Rate V, ×10 ⁻⁴ mM/min	Conversion, %
3a	1	23	2	2410	79
3a	5	23	2		99
3b	4	77	2	440	60
3b	14	77	2		99
3c	14	77	2	418	96
3a	48	23	1	n.d.	0
3a	24	23	F ^c	2.26	1
3a	24	23	F ^c + 1	2.87	1
3b	48	77	1	n.d.	1
3b	24	77	F ^c	4.03	6

^a[3a–c] = 12.3 mM, [H₂O] = 74 mM, CD₃CN; ^b[1/2] = 0.51 mM; ^c[F] = 3.08 mM, i.e., 6 equiv with respect to 2, to ensure the same number of acidic groups in the system.

showed 6% conversion after 24 h at 77 °C, with $V = 4.03 \times 10^{-4}$ mM/min. The rate enhancement provided by internalizing the acid groups in the cage cavity is 1070-fold for 3a, and 100-fold for 3b. Unfunctionalized cage 1 was not an effective catalyst: no solvolysis of acetals 3a, 3b or 3c occurred after 48 h with 4% cage 1 at 23 °C. When the samples were heated, minimal conversion (~1%) was observed after 24 h.

The rate enhancement is provided by the cage structure: while NMR analysis showed that 3a–c are in fast exchange with cage 2 and no discrete Michaelis complex is observed, the acetals do have significant affinity for the cage. Stern–Volmer analysis of the absorbance spectra (Supporting Information) illustrated this strong host:guest affinity, with $K_D(2\cdot3a) = 76 \mu\text{M}$ and $K_D(2\cdot3b) = 44 \mu\text{M}$. No binding was observed between 3a–c and control ligand F: the molecular recognition is driven by the multiple closely located acid groups and the cationic nature of the cage host. Interestingly, the unfunctionalized cage 1 also shows affinity for guests, with $K_D(1\cdot3c) = 10 \mu\text{M}$. It is an ineffective catalyst, however, as it has no reactive functional groups.

Cavity-containing catalysts have another advantage over small molecules: compartmentalization. This is important for tandem, or “cascade” catalysis,²² an example of which is shown in Figure 4. Cage-to-cage conversions of self-assembled M₂L₃ helicates such as 4•Br can occur under mild conditions by adding 2-formylpyridine and water to the system. Aldehyde exchange occurs only if the process is enthalpically favorable, i.e., if an electron-poor aldehyde is replaced by an electron rich aldehyde.²³ However, coupling this reaction to a tandem process is challenging, as the helicates are sensitive to acid, as well as carboxylate or chloride ions. To perform both a deprotection of the 2-formylpyridine acetal and the helicate aldehyde exchange requires careful matching of conditions. Stronger acids such as CF₃COOH are effective catalysts for acetal solvolysis, but also allow other side reactions to occur.

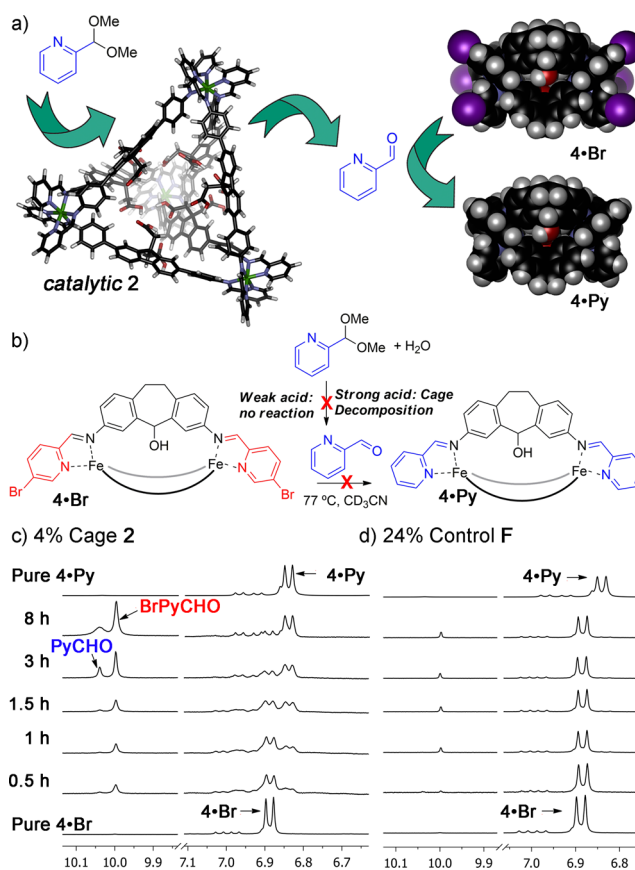


Figure 4. Tandem catalysis with (a) cage 2; (b) controls. ¹H NMR spectra of the tandem reaction of acetal 3b (12.3 mM) with helicate 4•Br (1.5 mM), H₂O (61.5 mM) and (c) cage 2 (0.51 mM); (d) acid F (3.08 mM), CD₃CN, 77 °C.

Weak acids do not destroy the helicates but are ineffective in deprotecting the acetal.

Acid cage 2 is perfectly suited to this tandem process. 4% cage 2 was combined with 3b, water, and brominated helicate 4•Br in CD₃CN, and the tandem process monitored at 77 °C (Figure 4c, Supporting Information). The solvolysis of 3b and the incorporation of the resultant PyCHO into 4•Br occur rapidly: after only 30 min, peaks for 4•Br start to disappear. Peaks for PyCHO are not observed initially, only peaks for displaced BrPyCHO. As an excess of the acetal is present, excess PyCHO builds up after 3 h. The reaction achieves completion after 8 h, with a conversion of 92%. No decomposition of the helicates occurs, and only the helicates, 2 and excess aldehydes are present after the reaction. No incorporation of BrPyCHO into cage 2 is observed, as expected: even though 2 is an iminopyridine cage, it is capable of catalyzing the displacement reactions of other iminopyridine assemblies.

Cage 2 is a good catalyst for this tandem solvolysis/displacement, whereas other acids are not (Figure 4d, Supporting Information). No acetal solvolysis is observed with control acid F after 8 h, and decomposition of 4•Br occurs after extended heating (120 h). Using a stronger acid such as CF₃CO₂H led to rapid decomposition after only 10 min at 77 °C. Acetal solvolysis was observed, but the helicates were not tolerant of the strong acid, even at 23 °C. When cage 1 was used as catalyst, no acetal solvolysis occurred, and 4•Br persisted even after extended reaction. The combination of

enhanced reactivity and compartmentalization of the acid groups in cage 2 allows it to be an effective tandem catalyst: reactive enough to be functional, but mild enough to work with sensitive tandem partners.

In conclusion, we have shown that an endohedrally functionalized cage complex is capable of 1000-fold accelerations of acid-catalyzed reactions over nonassembled control acids, and this can be applied to tandem cage-to-cage interconversions. The cage binds substrate strongly, and releases the products rapidly, allowing good turnover. The internally functionalized cage allows sequestration of reactive species, reaction rate accelerations and concurrent tandem reactions: the hallmarks of enzymatic catalysis.

■ ASSOCIATED CONTENT

Supporting Information

The Supporting Information is available free of charge on the ACS Publications website at DOI: 10.1021/jacs.8b03984.

New molecule synthesis, cage characterization and assignment (PDF)

■ AUTHOR INFORMATION

Corresponding Author

*richard.hooley@ucr.edu

ORCID

Ryan R. Julian: 0000-0003-1580-8355

Richard J. Hooley: 0000-0003-0033-8653

Notes

The authors declare no competing financial interest.

■ ACKNOWLEDGMENTS

The authors thank the National Science Foundation (CHE-1708019 to R.J.H.) and NIH (NIGMS grant R01GM107099 to R.R.J.) for funding.

■ REFERENCES

- (1) (a) Brown, C. J.; Toste, F. D.; Bergman, R. G.; Raymond, K. N. *Chem. Rev.* **2015**, *115*, 3012–3035. (b) Ward, M. D.; Raithby, P. R. *Chem. Soc. Rev.* **2013**, *42*, 1619–1636. (c) Cook, T. R.; Stang, P. J. *Chem. Rev.* **2015**, *115*, 7001–7045. (d) Chakrabarty, R.; Mukherjee, P. S.; Stang, P. J. *Chem. Rev.* **2011**, *111*, 6810–6918.
- (2) Kang, J. M.; Rebek, J., Jr. *Nature* **1997**, *385*, 50–52.
- (3) Kaanumalle, L. S.; Gibb, C. L. D.; Gibb, B. C.; Ramamurthy, V. J. *Am. Chem. Soc.* **2005**, *127*, 3674–3675.
- (4) (a) Pluth, M. D.; Bergman, R. G.; Raymond, K. N. *Science* **2007**, *316*, 85–88. (b) Hastings, C. J.; Fiedler, D.; Bergman, R. G.; Raymond, K. N. *J. Am. Chem. Soc.* **2008**, *130*, 10977–10988. (c) Lee, S. J.; Cho, S.-H.; Mulfort, K. L.; Tiede, D. M.; Hupp, J. T.; Nguyen, S. T. *J. Am. Chem. Soc.* **2008**, *130*, 16828–16829. (d) Hastings, C. J.; Pluth, M. D.; Bergman, R. G.; Raymond, K. N. *J. Am. Chem. Soc.* **2010**, *132*, 6938–6940. (e) Wang, J. Z.; Brown, C. J.; Bergman, R. G.; Raymond, K. N.; Toste, F. D. *J. Am. Chem. Soc.* **2011**, *133*, 7358–7360. (f) Murase, T.; Nishijima, Y.; Fujita, M. *J. Am. Chem. Soc.* **2012**, *134*, 162–164. (g) Bolliger, J. L.; Belenguer, A. M.; Nitschke, J. R. *Angew. Chem., Int. Ed.* **2013**, *52*, 7958–7962. (h) Salles, A. G.; Zarra, S.; Turner, R. M.; Nitschke, J. R. *J. Am. Chem. Soc.* **2013**, *135*, 19143–19146. (i) Kohyama, Y.; Murase, T.; Fujita, M. *J. Am. Chem. Soc.* **2014**, *136*, 2966–2969. (j) Jiao, J.; Tan, C.; Li, Z.; Liu, Y.; Han, X.; Cui, Y. *J. Am. Chem. Soc.* **2018**, *140*, 2251–2259.
- (5) (a) Leung, D. H.; Fiedler, D.; Bergman, R. G.; Raymond, K. N. *Angew. Chem., Int. Ed.* **2004**, *43*, 963–966. (b) Leung, D. H.; Bergman, R. G.; Raymond, K. N. *J. Am. Chem. Soc.* **2006**, *128*, 9781–9797. (c) Levin, M. D.; Kaphan, D. M.; Hong, C. M.; Bergman, R. G.; Raymond, K. N.; Toste, F. D. *J. Am. Chem. Soc.* **2016**, *138*, 9682–

9693. (d) Kaphan, D. M.; Levin, M. D.; Bergman, R. G.; Raymond, K. N.; Toste, F. D. *Science* **2015**, *350*, 1235–1238. (e) Nishioka, Y.; Yamaguchi, T.; Yoshizawa, M.; Fujita, M. *J. Am. Chem. Soc.* **2007**, *129*, 7000–7001. (f) Yoshizawa, M.; Tamura, M.; Fujita, M. *Science* **2006**, *312*, 251–254.
- (6) Zhao, C.; Toste, F. D.; Bergman, R. G.; Raymond, K. N. *J. Am. Chem. Soc.* **2014**, *136*, 14409–14412.
- (7) (a) Cullen, W.; Misuraca, M. C.; Hunter, C. A.; Williams, N. H.; Ward, M. D. *Nat. Chem.* **2016**, *8*, 231–236. (b) Cullen, W.; Metherell, A. J.; Wragg, A. B.; Taylor, C. G. P.; Williams, N. H.; Ward, M. D. *J. Am. Chem. Soc.* **2018**, *140*, 2821–2828.
- (8) Martí-Centelles, V.; Lawrence, A. L.; Lusby, P. J. *J. Am. Chem. Soc.* **2018**, *140*, 2862–2868.
- (9) Wasilke, J.-C.; Obrey, S. J.; Baker, R. T.; Bazan, G. C. *Chem. Rev.* **2005**, *105*, 1001–1020.
- (10) (a) Suzuki, K.; Iida, J.; Sato, S.; Kawano, M.; Fujita, M. *Angew. Chem., Int. Ed.* **2008**, *47*, 5780–5782. (b) Suzuki, K.; Kawano, M.; Sato, S.; Fujita, M. *J. Am. Chem. Soc.* **2007**, *129*, 10652–10653. (c) Sato, S.; Ishido, Y.; Fujita, M. *J. Am. Chem. Soc.* **2009**, *131*, 6064–6065. (d) Fujita, D.; Suzuki, K.; Sato, S.; Yagi-Utsumi, M.; Yamaguchi, Y.; Mizuno, N.; Kumasaka, T.; Takata, M.; Noda, M.; Uchiyama, S.; Kato, K.; Fujita, M. *Nat. Commun.* **2012**, *3*, 2093–2099.
- (11) (a) Wang, Q.-Q.; Gonell, S.; Leenders, S. H. A. M.; Dürr, M.; Ivanović-Burmazović, I.; Reek, J. N. H. *Nat. Chem.* **2016**, *8*, 225–230. (b) Gramage-Doria, R.; Hessels, J.; Leenders, S. H. A. M.; Tröppner, O.; Dürr, M.; Ivanović-Burmazović, I.; Reek, J. N. H. *Angew. Chem., Int. Ed.* **2014**, *53*, 13380–13384.
- (12) Dai, F.-R.; Wang, Z. *J. Am. Chem. Soc.* **2012**, *134*, 8002–8005.
- (13) Qiao, Y.; Zhang, L.; Li, J.; Lin, W.; Wang, Z. *Angew. Chem., Int. Ed.* **2016**, *55*, 12778–12782.
- (14) Lee, J.; Farha, O. K.; Roberts, J.; Scheidt, K. A.; Nguyen, S. T.; Hupp, J. T. *Chem. Soc. Rev.* **2009**, *38*, 1450–1459.
- (15) Mal, P.; Schultz, D.; Beyeh, K.; Rissanen, K.; Nitschke, J. R. *Angew. Chem., Int. Ed.* **2008**, *47*, 8297–8301.
- (16) Young, M. C.; Johnson, A. M.; Hooley, R. J. *Chem. Commun.* **2014**, *50*, 1378–1380.
- (17) Caulder, D. L.; Raymond, K. N. *Acc. Chem. Res.* **1999**, *32*, 975–982.
- (18) Holloway, L. R.; Bogie, P. M.; Lyon, Y.; Julian, R. R.; Hooley, R. J. *Inorg. Chem.* **2017**, *56*, 11435–11442.
- (19) (a) Meng, W.; Clegg, J. K.; Thoburn, J. D.; Nitschke, J. R. *J. Am. Chem. Soc.* **2011**, *133*, 13652–13660. (b) Ronson, T. K.; Meng, W.; Nitschke, J. R. *J. Am. Chem. Soc.* **2017**, *139*, 9698–9707.
- (20) Young, M. C.; Holloway, L. R.; Johnson, A. M.; Hooley, R. J. *Angew. Chem., Int. Ed.* **2014**, *53*, 9832–9836.
- (21) Ma, S.; Smulders, M. M. J.; Hristova, Y.; Clegg, J. K.; Ronson, T. K.; Zarra, S.; Nitschke, J. R. *J. Am. Chem. Soc.* **2013**, *135*, 5678–5684.
- (22) Ueda, Y.; Ito, H.; Fujita, D.; Fujita, M. *J. Am. Chem. Soc.* **2017**, *139*, 6090–6093.
- (23) Wiley, C. A.; Holloway, L. R.; Miller, T. F.; Lyon, Y.; Julian, R. R.; Hooley, R. J. *Inorg. Chem.* **2016**, *55*, 9805–9815.